photonics

MDPI

Article

Effects of Pulsed Red and Near-Infrared Light on Neuroblastoma Cells—Pilot Study on Frequency and Duty Cycle

Luyao Tang [1], Haokuan Qin [2], Shangfei Lin [2] and Muqing Liu [1,3,*]

[1] Department of Light Sources and Illuminating Engineering, Fudan University, 2005th Songhu Road, Shanghai 200441, China
[2] Institute of Future Lighting, Academy for Engineering and Technology, Fudan University, 220th Handan Road, Shanghai 200433, China
[3] Zhongshan Fudan Joint Innovation Center, 6th Xiangxing Road, Zhongshan 528403, China
* Correspondence: mqliu@fudan.edu.cn

Abstract: Transcranial photobiomodulation (tPBM) is an innovative intervention for a wide range of neurological and psychological conditions. tPBM therapy can enhance the metabolic capacity of neurons and bring about a variety of beneficial changes. This study mainly investigated the photobiological effects of pulsed red and near-infrared (NIR) light on neuron-like neuroblastoma SH-SY5Y cells by in vitro experiments. We covered the irradiation parameters, including wavelength (660, 850 nm), power density (5, 10, 20, 50, 100 mW/cm^2), frequency (40, 100, 1000 Hz), and duty cycle (10%, 50%, 90%), finding that pulsed light generated a distinct effect compared with continuous-wave light on the cellular responses. Cell viability, mitochondrial membrane potential (MMP), adenosine triphosphate (ATP), and reactive oxygen species (ROS) showed significant increase after irradiation of the adequate fluence amount (4.8–9.6 J/cm^2), and the enhancement was more notable under 40 Hz pulsed lighting. Under pulsed lighting with an average power density of 10 mW/cm^2, cells that received irradiation of higher peak power density up to 100 mW/cm^2 with a 10% duty cycle showed slightly higher metabolic responses. In addition, it was found that under same total fluence, short-term irradiation with high power density was more effective than long-term irradiation with low power density, which indicated the existence of a threshold to achieve effectiveness.

Keywords: tPBM; SH-SY5Y; pulsed light; ROS; cell viability; MMP; ATP

Citation: Tang, L.; Qin, H.; Lin, S.; Liu, M. Effects of Pulsed Red and Near-Infrared Light on Neuroblastoma Cells—Pilot Study on Frequency and Duty Cycle. *Photonics* **2023**, *10*, 315. https://doi.org/10.3390/photonics10030315

Received: 29 December 2022
Revised: 25 February 2023
Accepted: 6 March 2023
Published: 15 March 2023

1. Introduction

Photobiomodulation (PBM), also known as low-level light therapy (LLLT), has been proposed to be a noninvasive method that intervenes in a wide range of biological processes including the enhancement of energy production, gene expression, the prevention of cell death, and so on [1]. Its underlying mechanism is the non-thermal photon interaction of incident light with atoms or molecules in the cells and tissues [2]. PBM therapy is a form of treatment involving irradiating selected light on the target area of the human body in order to obtain beneficial effects, such as pain attenuation, wound healing, neurological disorder improvement, etc.

Recent studies have shown that transcranial photobiomodulation (tPBM) can modulate biological processes in the central nervous system [3–5]. The use of red to near-infrared (NIR) light in brain PBM therapy is a new method for treating a variety of neurological and psychological disorders. Cytochrome c oxidase (CCO) is considered to be the main photon receiver in the brain during the tPBM process. CCO is the terminal enzyme of the electron transport chain situated in the outer mitochondrial membrane, and is associated with energy generation within the mitochondria; thus, it has a potential therapeutic effect [6]. The absorption of the photons delivered through tPBM can increase the availability of electrons for the reduction of molecular oxygen in the catalytic center of CCO, causing increasing levels of mitochondrial membrane potential (MMP), adenosine triphosphate

(ATP), cyclic adenosine monophosphate (cAMP), and reactive oxygen species (ROS) [7]. To sum up, red or NIR irradiation can promote mitochondrial function, and can trigger the initiation of cellular signaling pathways [8].

The optimal parameters of brain PBM therapy, such as wavelength, fluence, power density, the number of repetitions, and the duration of treatment, have been variously investigated in preclinical studies [9]. However, research on the mode of light delivery (continuous or pulsed) is still not sufficient. Figure 1 and Table 1 provide brief explanations of the parameters applied when describing pulsed-wave (PW) light. It is proposed that the switching frequency of the potassium and calcium ion channels involved in the cellular response to PBM may be related to pulsed light. Further, PW light might dissociate more nitric oxide (NO) from CCO than continuous-wave (CW) light does during photodissociation [10]. In the general PBM field, Brondon et al. studied the pulsing influences on human HEP-2 cells, finding that 100 and 600 Hz pulsed light stimulated cell proliferation and oxidative burst maximally compared with CW light [11]. Ueda and Shimizu found that low-frequency pulsed laser irradiation significantly stimulated bone nodule formation in rat calvariae cells [12]. In the brain PBM field, the literature has shown that PW and CW light have different impacts on brain oscillation power [13], Alzheimer's disease [14], Parkinson's disease [15], etc. However, studies concerning pulsed light's impact on neurons or neuron-like cells are still lacking.

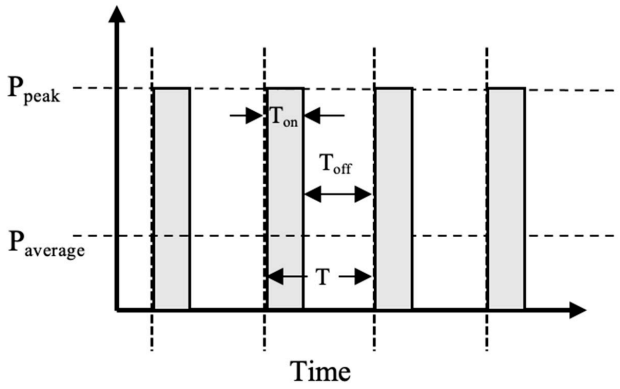

Figure 1. Parameters for describing pulsed light.

Table 1. Pulsed light parameters explanation.

Parameter	Unit	Description	Calculating Formula
T_{on}	s	The "on" time of the pulse interval duration	
T_{off}	s	The "off" time of the pulse interval duration	
T	s	The time duration of one-pulse interval	$T = T_{on} + T_{off}$
Frequency (f)	Hz	The number of pulse intervals per unit of time	$f = 1/T$
Duty cycle (D)	%	A unitless fractional number or % standing for the proportion of pulse-on time in each pulse interval	$D = T_{on}/T$
Power density	mW/cm^2	The intensity of power delivered per unit area and time	
Peak power density (P_{peak})	mW/cm^2	The power density of the "on" time of the pulse	
Average power density ($P_{average}$)	mW/cm^2	The mean power density of the pulse interval duration	$P_{average} = P_{peak} \times D$
Fluence	J/cm^2	The accumulated power delivered during the treatment per unit irradiation area	Fluence = $P_{average}$ × Irradiation Time
Dose	J	The accumulated power delivered during the treatment	Dose = Fluence × Irradiation area

The present study aimed to study the effects of PBM lighting on several cellular processes in neuron-like neuroblastoma SH-SY5Y cells. We selected cell viability, ROS production, MMP, and ATP levels as cellular indicators. The wavelengths of lighting were 660 and 850 nm since light in the spectral bands 650–680 and 800–870 nm matches the action spectrum of CCO [16] and has been confirmed to be effective in cognitive improvement in previous studies [17,18]. After a power density experiment (5, 10, 20, 50, 100 mW/cm^2), we specifically explored the effects of pulsed red/NIR light with various frequencies (40, 100, and 1000 Hz) and duty cycles (50%, 20%, and 10%), and the intervention time was 8 min. The chosen parameters of lighting were basically based on the experimental design of previous tPBM interventions. Barrett et al. [19] and Holmes et al. [20] designed a tPBM therapy with an 8 min duration and found significantly improved cognitive ability in healthy subjects. Zomorrodi et al. [13] found that 40 Hz pulsed light irradiating on the head could promote brain connectivity. Pulsed light of 100 Hz and 1000 Hz has been proved effective in improving behavioral performance in a rabbit stroke model [21].

In the past, most tPBM therapies were conducted with a laser, which makes it difficult to generate freely adjustable pulsed light. Recently, using a light-emitting diode (LED) has become an emerging trend in the field of tPBM. A LED is a semiconductor device whose light principle is different from that of lasers. When an electric current flows through it, the electrons recombine with holes and emit light that we need [22]. Due to its driving principle, LED can produce pulsed light with modulations in frequency and the duty cycle easily [23]. In addition, LED is smaller, lighter, and far less expensive than lasers, making it more suitable for home use.

2. Materials and Methods

2.1. Cell Culture

The study was approved by the Ethical Committee of Fudan University of Biology Sciences. Human neuroblastoma SH-SY5Y cells were obtained from a cell bank (Sunn-cell, Wuhan, China) and passed cell line STR authentication before delivery. The cells were cultured in DMEM/F12 (Gibco, Logan, UT, USA) containing 10% heat-inactivated fetal bovine serum (Gibco, Logan, UT, USA) and 1% streptomycin and penicillin (HyClone, Logan, UT, USA). The cells were maintained in 5% CO_2 and 95% air at 37 °C in a humidified incubator (Qiqian, Shanghai, China). One day before light irradiation, the SH-SY5Y cells were transferred to 96-well plates containing 150 µL of the medium/well, and seeded at a density of 5×10^3 cells/well [24].

2.2. Light Irradiation

The light source was LEDs emitting at 660 and 850 nm (Samsung, Seoul, Republic of Korea), and the irradiation was performed in a humidified incubator (LightEngin Technology, Shanghai, China) (Figure 2a). The lighting device was on top of the incubator and could be replaced for different wavelengths needs. The power density was measured by an optical power meter (Thorlabs, Newtown, CT, USA). The spectra of the 660 and 850 nm LEDs are shown in Figure 2b.

A total of 24 h before the irradiation, proper numbers of 96-well plates were prepared according to the design of the experimental conditions. Each plate would only accept one kind of lighting condition. Generally, the cells were located in the center of the 96-hole board, as shown in Figure 3. In the actual experiments, we prepared 6 replicate wells for CCK-8 tests and 4 replicate wells for ROS, MMP, and ATP measurement each time. One 96-well plate only received one lighting condition and completed the measurement of one indicator (cell viability, ROS, MMP, or ATP) each time. Plates in the control group did not receive any light irradiation, but they still needed to be placed in the lighting incubator like the other groups. All the experiments were repeated three times independently.

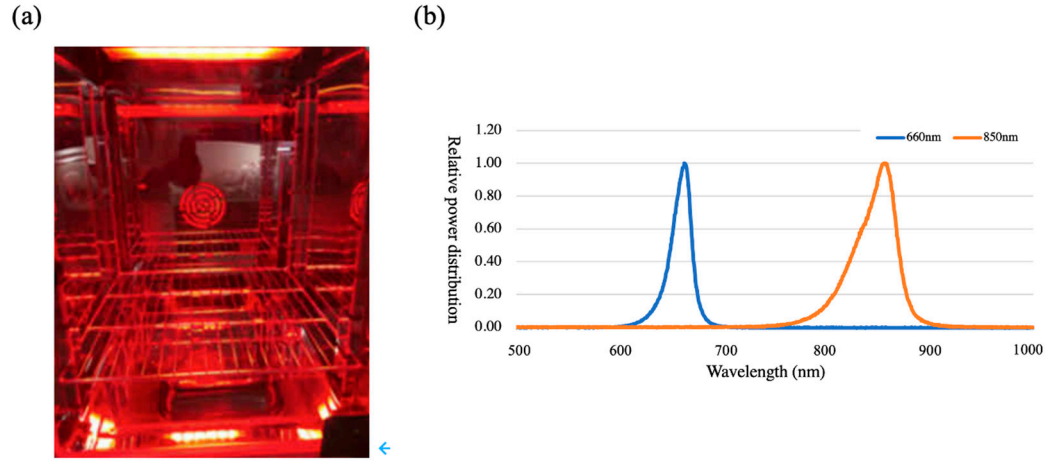

Figure 2. Light-humidified incubator and spectrum of the respective LED light source. (**a**) Light humidified incubator. (**b**) The spectra of red light (660 nm) and NIR light (850 nm) used in this study.

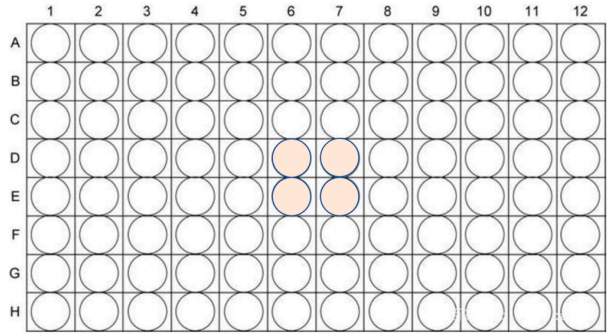

Figure 3. Layout of duplicated wells (marked in pink) in 96-well plate.

2.3. Lighting Parameters

In this study, we designed three experiments, focusing on power density, frequency, and duty cycle, respectively.

2.3.1. Experiment 1: Power Density

In Experiment 1, we studied the CW mode, unified the lighting time to 8 min, and set 5 different power densities: 5, 10, 20, 50, and 100 mW/cm^2. The corresponding fluence values were 2.4, 4.8, 9.6, 24, and 48 J/cm^2. The purpose of Experiment 1 was to investigate the impact of fluence and further determine the optimal choice for the subsequent pulsed-light experiments. The lighting parameters are shown in Table 2.

Table 2. Experimental conditions for intensity experiment.

Group	Operation Mode	Power Density	Irradiation Time	Fluence
Control		/		
660 nm	CW	5 mW/cm^2	8 min	2.4 J/cm^2
	CW	10 mW/cm^2		4.8 J/cm^2
	CW	20 mW/cm^2		9.6 J/cm^2
	CW	50 mW/cm^2		24 J/cm^2
	CW	100 mW/cm^2		48 J/cm^2
850 nm	CW	5 mW/cm^2		2.4 J/cm^2
	CW	10 mW/cm^2		4.8 J/cm^2
	CW	20 mW/cm^2		9.6 J/cm^2
	CW	50 mW/cm^2		24 J/cm^2
	CW	100 mW/cm^2		48 J/cm^2

2.3.2. Experiment 2: Frequency

Experiment 2 focused on exploring the effects of pulsed light's frequency on cells. We chose 40, 100, and 1000 Hz as the variables. The treatment time was still fixed at 8 min, and the average power density was set to 10 mW/cm^2. Since the $P_{average}$ was the same, the total fluence was also the same, which was fixed at 4.8 J/cm^2. The lighting parameters are shown in Table 3.

Table 3. Experimental conditions for frequency experiment.

Group	Operation Mode			$P_{average}$	Irradiation Time	Fluence
Control				/		
660 nm	CW			10 mW/cm^2	8 min	4.8 J/cm^2
	PW					
	Frequency	Duty cycle	P_{peak}			
	40 Hz	50%	20 mW/cm^2			
	100 Hz	50%	20 mW/cm^2			
	1000 Hz	50%	20 mW/cm^2			
850 nm	CW					
	PW					
	Frequency	Duty cycle	P_{peak}			
	40 Hz	50%	20 mW/cm^2			
	100 Hz	50%	20 mW/cm^2			
	1000 Hz	50%	20 mW/cm^2			

2.3.3. Experiment 3: Duty Cycle

Experiment 3 focused on exploring the effects of pulsed light's duty cycle. The illumination time was still fixed at 8 min, and the average power density was set to 10 mW/cm^2. The duty cycle was set to 50%, 20%, and 10%, and the corresponding peak power densities were 20, 50, and 100 mW/cm^2. We chose 40 Hz as the fixed frequency, and the lighting parameters are shown in Table 4.

Table 4. Experimental conditions for duty cycle.

Group	Operation Mode			$P_{average}$	Irradiation Time	Fluence
Control				/		
660 nm	CW			10 mW/cm^2	8 min	4.8 J/cm^2
	PW					
	Frequency	Duty cycle	P_{peak}			
	40 Hz	10%	100 mW/cm^2			
	40 Hz	20%	50 mW/cm^2			
	40 Hz	50%	20 mW/cm^2			
850 nm	CW					
	PW					
	Frequency	Duty cycle	P_{peak}			
	40 Hz	10%	100 mW/cm^2			
	40 Hz	20%	50 mW/cm^2			
	40 Hz	50%	20 mW/cm^2			

2.4. Measurement of Cell Viability

Cell viability was assessed with a CCK-8 reagent (Dojindo Laboratories, Kumamoto, Japan) 24 h after light irradiation. When testing, the original medium was aspirated, and 110 µL/well of the mixed solution containing 90% of the serum-free medium and 10% of the CCK-8 reagent was added. The absorbance value at 450 nm was read with a 96-well plate reader (Multiskan FC, Thermo Scientific, Waltham, MA, USA).

2.5. Measurement of Intracellular ROS

The level of intracellular ROS was measured using the fluorescence probe DCFH-DA (Beyotime, Shanghai, China). ROS was detected immediately after light irradiation. At the indicated time, the original medium was aspirated, and 100 µL/well of a mixed solution containing the serum-free medium and DCFH-DA (2000:1) was added. The cells were then incubated with the mixed solution at 37 °C for 10 min, and were washed with PBS after incubation. A fluorescence microscope (BX53, Olympus Life Science, Tokyo, Japan) at an emission wavelength of 500 nm was used for observation.

2.6. Measurement of Mitochondrial Membrane Potential

The mitochondrial membrane potential kit with JC-1 (Jiancheng, Nanjing, China) was used to detect the MMP. The measurement was conducted immediately after the light delivery. The cells were incubated with a JC-1 fluorescent probe at 37 °C for 20 min, were washed one time with a JC-1 (1×) buffer, and were observed with the fluorescence microscope at an emission wavelength of 510 nm and 580 nm.

2.7. Measurement of ATP

CellTiter-Glo Luminescent Cell Viability Assay (Promega, Madison, WI, USA) was used to measure the ATP level 10 min after light application [25]. This assay generates a "glow-type" luminescent signal produced by a luciferase reaction with cellular ATP. The Cell Titer-Glo reagent was added in an amount equal to the volume of the medium (150 µL/well) and resulted in cell lysis followed by a sustained luminescent reaction that was measured using a reporter luminometer (Synergy™ 2, BioTek, Winooski, VT, USA). The amounts of ATP present in the SH-SY5Y cells were quantified in relative luminescent units (RLUs) by the luminometer in each well.

2.8. Statistical Analysis

The data were analyzed and expressed as mean ± standard deviation. Significant differences between the groups were compared using the one-way ANOVA with a Tukey's post hoc test, and the differences were considered statistically significant at * $p < 0.05$ and ** $p < 0.01$.

3. Results

3.1. Experiment 1: Power Density

The results presented in Figure 4 show that the red/NIR lighting effects on SH-SY5Y cells are sensitive to the fluence and power density, displaying a generally rising and then falling trend, except for ROS. At a power density of 10 mW/cm^2, SH-SY5Y viability rose the most, by 11.7% after a 660 nm irradiation and by 7.3% after an 850 nm irradiation (Figure 4a). At a power density of 20 mW/cm^2, ATP increased most notably, by 24.5% under 660 nm irradiation and 15.7% under 850 nm irradiation (Figure 4b). MMP showed a similar pattern to ATP, increasing by 21.7% and 20.4% under each irradiation, respectively (Figure 4d). ROS exhibited a bimodal pattern at 20 and 100 mW/cm^2 (Figures 4c and 5), which is similar to the previous ROS production results of mouse primary cortical neurons after an 810 nm laser irradiation [7].

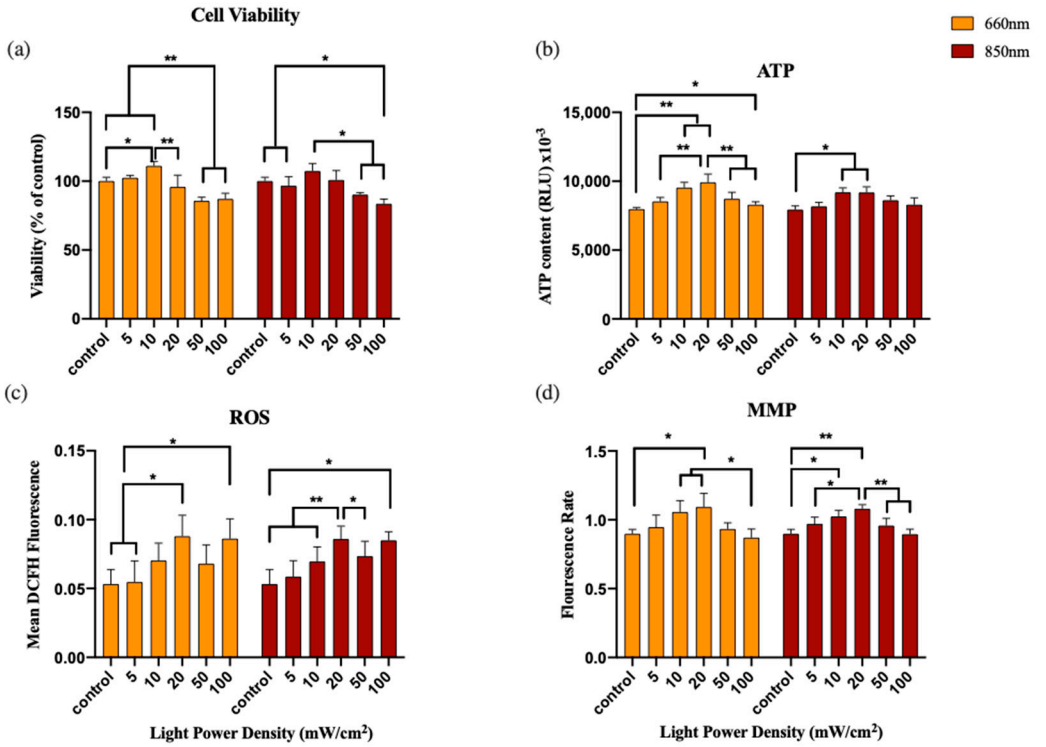

Figure 4. Comparison between control and CW light with different power densities: (**a**) cell Viability, (**b**) ATP, (**c**) ROS, and (**d**) MMP. * $p < 0.05$ and ** $p < 0.01$.

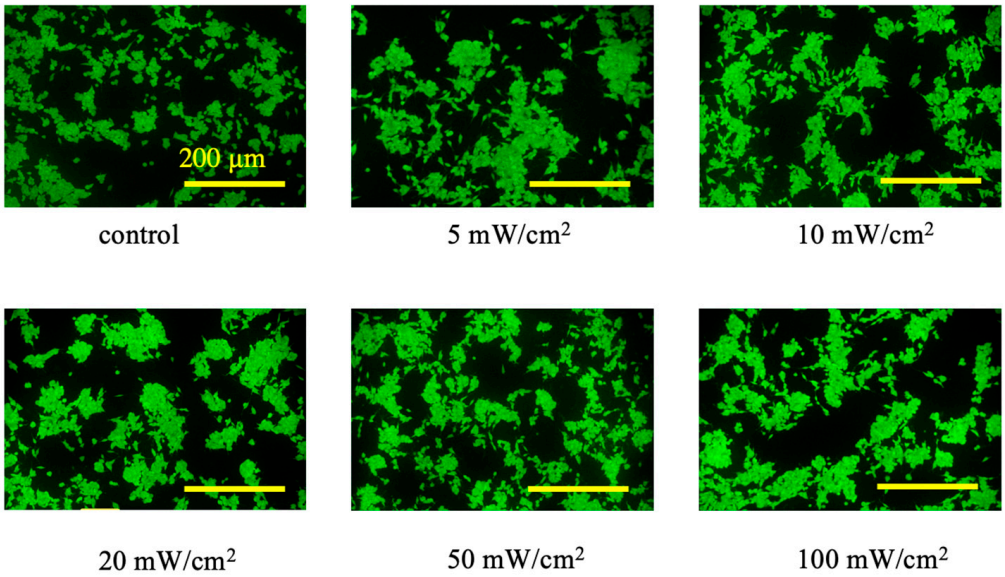

Figure 5. ROS of control and CW light groups with different power densities, showing an interesting triphasic pattern.

3.2. Experiment 2: Frequency

Results of the frequency experiment are shown in Figure 6. It can be found that the cell viability, ATP and MMP levels of 40 Hz PW light group were significantly different from the control group under 660 nm and 850 nm irradiation, so is ROS level under 850 nm lighting. In addition, the 1000 Hz PW group of 660 nm and 850 nm both showed significant differences in ATP levels compared with the control group (Figure 6b). This indicates that at the cellular level, the effect of pulsed light is sensitive to frequency.

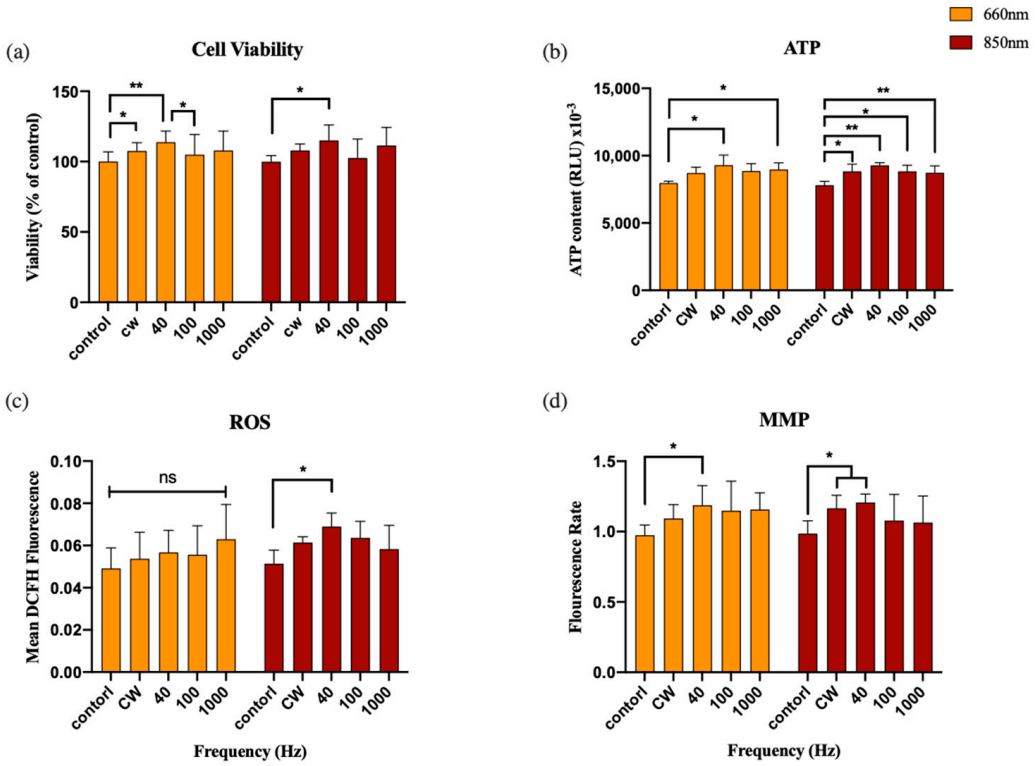

Figure 6. Comparison between control, CW, and PW light groups with different frequencies: (**a**) cell Viability, (**b**) ATP, (**c**) ROS, and (**d**) MMP. * $p < 0.05$ and ** $p < 0.01$; *ns: not significant*.

3.3. Experiment 3: Duty Cycle

From the results shown in Figure 7, we can tell that the results of the 20% and 10% duty cycle group were generally higher than those of the control and the 50% group. The ATP levels of the 20% and 10% duty cycle groups were about 23% significantly higher than those of the control group and 8% significantly higher than that of the 50% duty cycle group under 660 nm lighting (Figure 7b). The MMP result of the 10% duty cycle group was 13.3%, which is significantly higher than that of the 50% duty cycle group under 660 nm irradiation (Figure 7d). In summary, with the same $P_{average}$, a smaller duty cycle (which equals to a higher P_{peak}) would bring a slight boost in cell viability, ATP, ROS, and MMP levels.

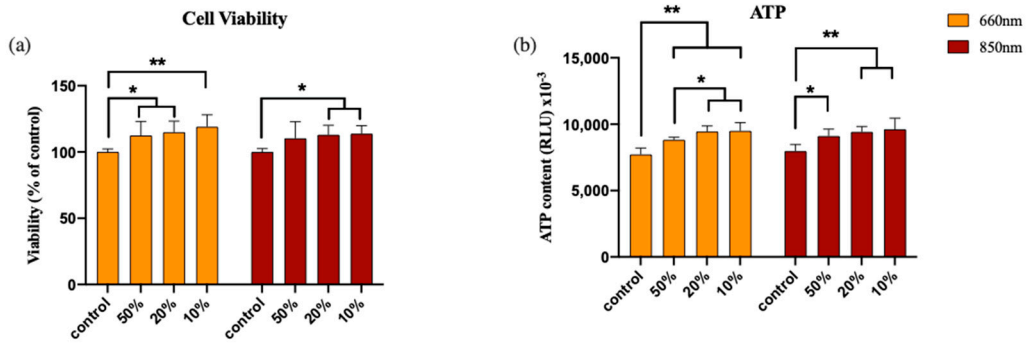

Figure 7. *Cont.*

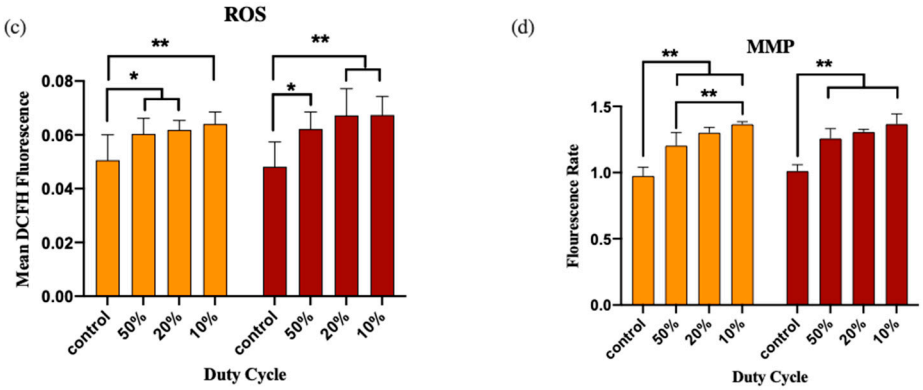

Figure 7. Comparison between control and PW light with different duty cycles: (**a**) cell viability, (**b**) ATP, (**c**) ROS, and (**d**) MMP. * $p < 0.05$ and ** $p < 0.01$.

4. Discussion

Over the past two decades, brain PBM therapy has gained increasing attention as an innovative method for stimulating neural activity [9]. Using red to NIR light, brain PBM can intervene in a wide range of neurological and psychological conditions. The optimal parameters, such as wavelength, dose, fluence, intensity, operation mode, repetition intervals, etc., have been variously investigated in previous studies. Some of the literature has reported the comparison of the PW and CW mode by in vivo [26–28] or preclinical experiments [13], but the study of PW-mode lighting at the cellular level is still lacking. Therefore, we designed this experiment to conduct a comparison between PW and CW light and mainly explored the effects of frequency and duty cycles.

4.1. Discussion on Parameters Optimization

The importance of lighting parameter optimization for achieving better intervention effects has been proved by the previous literature and data obtained on our own. A preliminary conclusion can be drawn that wavelength determines whether a beneficial effect exists, while power density, frequency, waveform, etc., determine the strength of the effect.

In Experiment 1, the obtained data showed that cell viability increased after low-dose fluences of light and decreased with excess fluence. These results indicate a biphasic effect [29], which is quite common in the field of PBM. A biphasic effect suggests that if insufficient energy is applied, there will be no response during PBM, but when too much energy is applied, then the stimulation disappears and is replaced by the inhibition effect instead. ROS generation presented a triphasic pattern in Experiment 1. We propose that light-induced ROS can be produced from mitochondria both when respiration is increased (beneficial), or alternatively when it is decreased (harmful). Respiration is decreased when mitochondria are damaged by excessive ROS, and in this situation, MMP and ATP decreased as a prelude to the induction of apoptosis (Figure 4b,d).

We found that there were no significant differences between the ATP and MMP results of the 10 mW/cm^2 and 20 mW/cm^2 groups in Experiment 1. The cell viability of the 10 mW/cm^2 group was higher than that of the 20 mW/cm^2 group, while the ROS of the 20 mW/cm^2 group was higher than that of the 10 mW/cm^2 group. Considering the human tPBM experimental design, we chose 10 mW/cm^2 as the baseline for our trials. Many previous tPBM studies have used 250 mW/cm^2 as the power density on the forehead [5,15–17]. Estimating the transmittance to be 4% [30], we calculated that the light power density reaching the cortex would be approximately 10 mW/cm^2. From this perspective, we think it is reasonable to choose 10 mW/cm^2 for our experiments.

From Experiment 2, we obtained 40 Hz as a better frequency choice. Similarly, Rosenberg et al. investigated cell proliferation and the markers of cell maturation and metabolic activity of cultured osteoblast-like cells following pulsed LED irradiance, finding that 40 Hz was the optimal parameter [31]. Furthermore, 40 Hz is a relatively common choice in the tPBM field. It is found that 40 Hz pulsed irradiation could increase brain connectivity [13]

and play an important role in reliving Alzheimer's disease-related symptoms [32]. The underlying mechanism of the optimal frequency is worthy of further investigation.

From Experiment 3, our data show that lighting generates slightly higher levels of metabolic responses as the duty cycle became smaller. A smaller duty cycle means a higher P_{peak} when the $P_{average}$ remains the same. To our knowledge, there is no prior research regarding the cellular response to different P_{peak} values, while the mechanism of this needs further investigation. Using PW light can obtain a greater P_{peak} than CW light can with the same $P_{average}$. During T_{on}, PW light can deliver a larger number of photons at any given depth, which means deeper penetration in tissues [33]. Meanwhile, because of the "quench periods" (T_{off}) following the pulse-on times, pulsed light may not cause thermal damage despite a higher P_{peak} [34].

As for the target cell selection, a normal-type neuron could be a better choice, but the purpose of investigating a wide range of parameters made us select SH-SY5Y in the end. It is easier to obtain a large quantity of cells with cell-line cells, and the cell state can be more stable and repetitive. A recent study conducted by Golovynska et al. demonstrated that the photobiological response trends of ROS, MMP, and the cell viability of neurons and neuroblastoma cells were similar to each other [35], so we think SH-SY5Y can help us reveal the regular pattern of neuron-type cells' responses to pulsed light.

4.2. Discussion on Power Density-Time Relationship

We noticed that in Golovynska et al.'s results [35], the cell viability of SH-SY5Y cells increased by 19, 23, 34, and 30% after 650 nm irradiation and by 15, 21, 29, and 31% after 808 nm irradiation at fluences of 3, 6, 12, and 30 J/cm^2, respectively [35]. They also found that when the total fluence reached 60 J/cm^2 or 120 J/cm^2, the cell viability decreased significantly. However, our results showed that when the total fluence reached 24 J/cm^2 and 48 J/cm^2, cell viability decreased. Compared with our settings, their power density was fixed at 100 mW/cm^2 and the irradiation time ranged from 10 s to 20 min. This caused our interest in exploring the power density–time relationship. We fixed the total fluence at 4.8 J/cm^2 (same as Experiment 2 and 3), and then changed the power density from 5, 10, 20, and 50 to 100 mW/cm^2, and the corresponding irradiation times were 16 min, 8 min, 4 min, 96 s, and 48 s, respectively. This is different from Experiment 1, since the irradiation time in Experiment 1 was fixed at 8 min and the total fluence varied. The results are shown in Figure 8, and it turned out that there existed a threshold (approximately 10 mW/cm^2) in this case, which means only light with a power density higher than 10 mW/cm^2 generated higher metabolism activity. On this basis, future tPBM therapies may increase the power density and reduce the irradiation time, while the total dose or fluence be controlled at the optimal level.

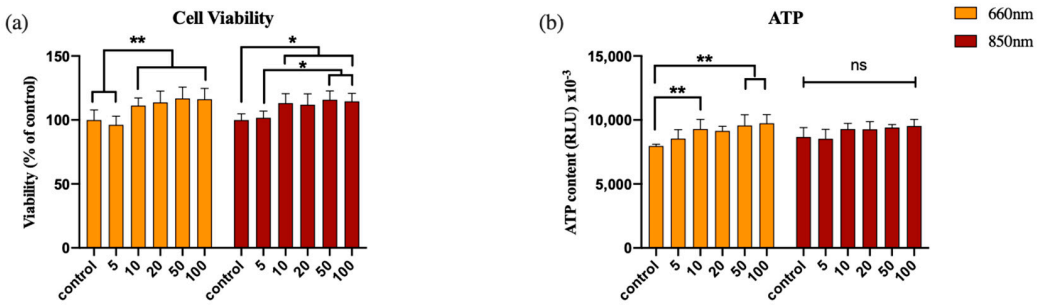

Figure 8. *Cont.*

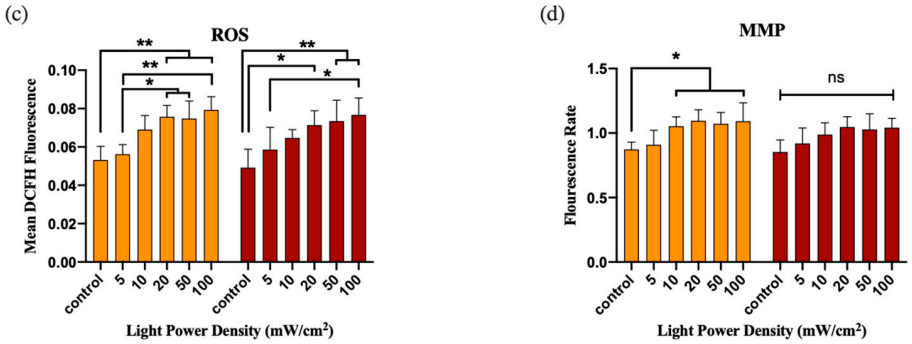

Figure 8. Comparison between CW light with different light power densities and fixed fluences: (**a**) cell viability, (**b**) ATP, (**c**) ROS, and (**d**) MMP. * $p < 0.05$ and ** $p < 0.01$. *ns: not significant*.

4.3. Discussion on ATP Level Increment

The redox changes in the CCO enzyme stimulate a transient alteration in the electrochemical potential of the mitochondrial membrane and bring about an increase in ATP. Sharma et al. tested the ATP of mouse primary cortical neurons after 5 min of 810 nm, 25 mW/cm^2 light irradiation. Their results showed that with a dose of 3 J, the amount of ATP was about two times higher than that of the control group [7]. Similarly, Oron et al. reported that GaAs (808 nm, 50 mW/cm^2, 1 s, 0.05 J/cm^2) laser irradiation enhanced ATP production in human neuronal progenitor cells [25]. They measured the ATP 10 min after irradiation and observed that the ATP production in the light group was double that in the control group. In our experiments, the increase in ATP, about 23% at most, was not doubled or even higher, and this may be attributed to the difference between neuroblastoma cells and neurons [35]. Another possible explanation is that we cooled the 96-well plate at room temperature for 30 min after irradiation according to the instructions for the CellTiter-Glo Luminescent Cell Viability Assay, and then carried out the fragmentation operation with a shaker. We then cooled the plate at room temperature for 10 min again (still referring to the instruction manual) before performing the luminescence measurement. In contrast, the waiting time in the previous literature is relatively short—about 5–10 min.

5. Conclusions

To sum up, this study utilized 660 nm and 850 nm LED lighting to conduct a relatively comprehensive study of the cellular response of SH-SY5Y cells, with regard to the power density, fluence, frequency, and duty cycle. It can be concluded that 10–20 mW/cm^2 light irradiation can promote metabolic response significantly. With the same $P_{average}$ (10 mW/cm^2), 40 Hz pulsed light with a 10% duty cycle (P_{peak} equals to 100 mW/cm^2) produced higher metabolic capacity on neuron-like cells. Our results showed that the frequency and duty cycle had a distinct impact on the cells, suggesting the potential importance of the PW mode in clinical trials. To the best of our knowledge, this is the first time that the effects of pulsed light on neuron-like cells has been revealed. Further research of pulsed light's effects on the intracellular level of Ca^{2+} ions, CCO oxidation reaction, and corresponding signaling pathways is worthy to be carried out.

Author Contributions: Conceptualization, L.T. and M.L.; methodology, L.T. and H.Q.; investigation, L.T. and S.L.; data curation, L.T.; writing—original draft preparation, L.T.; writing—review and editing, L.T. and M.L.; supervision, M.L.; All authors have read and agreed to the published version of the manuscript.

Funding: This work was supported by the Development of Various Medical Instruments Based on Pulsed Light program funded by the Zhongshan Municipal Government (Grant No. 15-BD-015).

Conflicts of Interest: The authors declare no conflict of interest.

References

1. Hamblin, M.R.; Agrawal, T.; de Sousa, M. *Handbook of Low-Level Laser Therapy*, 1st ed.; Jenny Stanford Publishing: Dubai, United Arab Emirates, 2016.
2. Chung, H.; Dai, T.; Sharma, S.K.; Huang, Y.Y.; Carroll, J.D.; Hamblin, M.R. The Nuts and Bolts of Low-Level Laser (Light) Therapy. *Ann. Biomed. Eng.* **2012**, *40*, 516–533. [CrossRef]
3. Lapchak, P.A.; Boitano, P.D. A Novel Method to Promote Behavioral Improvement and Enhance Mitochondrial Function Following an Embolic Stroke. *Brain Res.* **2016**, *120*, 670–683. [CrossRef] [PubMed]
4. Dong, T.; Zhang, Q.; Hamblin, M.R.; Wu, M.X. Low-Level Light in Combination with Metabolic Modulators for Effective Therapy of Injured Brain. *J. Cereb. Blood Flow Metab.* **2015**, *25*, 180–182. [CrossRef] [PubMed]
5. Schiffer, F.; Johnston, A.L.; Ravichandran, C.; Polcari, A.; Teicher, M.H.; Webb, R.H.; Hamblin, M.R. Psychological Benefits 2 and 4 Weeks after a Single Treatment with near Infrared Light to the Forehead: A Pilot Study of 10 Patients with Major Depression and Anxiety. *Behav. Brain Funct.* **2009**, *5*, 46. [CrossRef] [PubMed]
6. Hamblin, M.R.; Huang, Y.-Y. *Photobiomodulation in the Brain Low-Level Laser (Light) Therapy in Neurology and Neuroscience*; Nikki Levy: Boca Raton, FL, USA, 2019.
7. Mancebo, M.C.; Eisen, J.L.; Sibrava, N.J.; Dyck, I.R.; Rasmussen, S.A. Dose Response Effects of 810 Nm Laser Light on Mouse Primary Cortical Neurons. *Lasers Surg. Med.* **2011**, *43*, 851–859. [CrossRef]
8. De Freitas, L.F.; Hamblin, M.R. Proposed Mechanisms of Photobiomodulation or Low-Level Light Therapy. *IEEE J. Sel. Top. Quantum Electron.* **2016**, *22*, 348–364. [CrossRef]
9. Salehpour, F.; Mahmoudi, J.; Kamari, F.; Sadigh-Eteghad, S.; Rasta, S.H.; Hamblin, M.R. Brain Photobiomodulation Therapy: A Narrative Review. *Mol. Neurobiol.* **2018**, *55*, 6601–6636. [CrossRef]
10. Hashmi, J.T.; Huang, Y.Y.; Sharma, S.K.; Kurup, D.B.; De Taboada, L.; Carroll, J.D.; Hamblin, M.R. Effect of Pulsing in Low-Level Light Therapy. *Lasers Surg. Med.* **2010**, *42*, 450–466. [CrossRef]
11. Brondon, P.; Stadler, I.; Lanzafame, R.J. Pulsing Influences Photoradiation Outcomes in Cell Culture. *Lasers Surg. Med.* **2009**, *41*, 222–226. [CrossRef]
12. Ueda, Y.; Shimizu, N. Effects of Pulse Frequency of Low-Level Laser Therapy (LLLT) on Bone Nodule Formation in Rat Calvarial Cells. *J. Clin. Laser Med. Surg.* **2003**, *21*, 271–277. [CrossRef]
13. Zomorrodi, R.; Loheswaran, G.; Pushparaj, A.; Lim, L. Pulsed Near Infrared Transcranial and Intranasal Photobiomodulation Significantly Modulates Neural Oscillations: A Pilot Exploratory Study. *Sci. Rep.* **2019**, *9*, 6309. [CrossRef]
14. De Taboada, L.; Yu, J.; El-Amouri, S.; Gattoni-Celli, S.; Richieri, S.; McCarthy, T.; Streeter, J.; Kindy, M.S. Transcranial Laser Therapy Attenuates Amyloid-β Peptide Neuropathology in Amyloid-β Protein Precursor Transgenic Mice. *J. Alzheimer's Dis.* **2011**, *23*, 521–535. [CrossRef]
15. Reinhart, F.; El Massri, N.; Chabrol, C.; Cretallaz, C.; Johnstone, D.M.; Torres, N.; Darlot, F.; Costecalde, T.; Stone, J.; Mitrofanis, J.; et al. Intracranial Application of Near-Infrared Light in a Hemi-Parkinsonian Rat Model: The Impact on Behavior and Cell Survival. *J. Neurosurg.* **2016**, *124*, 1829–1841. [CrossRef]
16. Cooper, C.E.; Springett, R. Measurement of Cytochrome Oxidase and Mitochondrial Energetics by near–Infrared Spectroscopy. *Philos. Trans. R. Soc. B Biol. Sci.* **1997**, *352*, 669–676. [CrossRef] [PubMed]
17. Jahan, A.; Nazari, M.A.; Mahmoudi, J.; Salehpour, F.; Salimi, M.M. Transcranial Near-Infrared Photobiomodulation Could Modulate Brain Electrophysiological Features and Attentional Performance in Healthy Young Adults. *Lasers Med. Sci.* **2019**, *34*, 1193–1200. [CrossRef]
18. Rojas, J.C.; Bruchey, A.K.; Gonzalez-Lima, F. Low-Level Light Therapy Improves Cortical Metabolic Capacity and Memory Retention. *J. Alzheimer's Dis.* **2012**, *32*, 741–752. [CrossRef]
19. Barrett, D.W.; Gonzalez-Lima, F. Transcranial Infrared Laser Stimulation Produces Beneficial Cognitive and Emotional Effects in Humans. *Neuroscience* **2013**, *230*, 13–23. [CrossRef] [PubMed]
20. Holmes, E.; Barrett, D.W.; Saucedo, C.L.; O'Connor, P.; Liu, H.; Gonzalez-Lima, F. Cognitive Enhancement by Transcranial Photobiomodulation Is Associated With Cerebrovascular Oxygenation of the Prefrontal Cortex. *Front. Neurosci.* **2019**, *13*, 1129. [CrossRef] [PubMed]
21. Lapchak, P.A.; Salgado, K.F.; Chao, C.H.; Zivin, J.A. Transcranial Near-Infrared Light Therapy Improves Motor Function Following Embolic Strokes in Rabbits: An Extended Therapeutic Window Study Using Continuous and Pulse Frequency Delivery Modes. *Neuroscience* **2007**, *148*, 907–914. [CrossRef]
22. Khanh, T.Q.; Bodrogi, P.; Vinh, Q.T.; Winkler, H. *LED Lighting: Technology and Perception*; John Wiley & Sons: Hoboken, NJ, USA, 2014.
23. Loo, K.; Lun, W.; Tan, S.; Lai, Y.; Tse, C. On Driving Techniques for LEDs: Toward a Generalized Methodology. *IEEE Trans. Power Electron.* **2009**, *24*, 2967–2976. [CrossRef]
24. Meng, C.; He, Z.; Xing, D. Low-Level Laser Therapy Rescues Dendrite Atrophy via Upregulating BDNF Expression: Implications for Alzheimer's Disease. *J. Neurosci.* **2013**, *33*, 13505–13517. [CrossRef] [PubMed]
25. Oron, U.; Ilic, S.; De Taboada, L.; Streeter, J. Ga-As (808 Nm) Laser Irradiation Enhances ATP Production in Human Neuronal Cells in Culture. *Photomed. Laser Surg.* **2007**, *25*, 180–182. [CrossRef] [PubMed]
26. Grillo, S.L.; Duggett, N.A.; Ennaceur, A.; Chazot, P.L. Non-Invasive Infra-Red Therapy (1072 Nm) Reduces β-Amyloid Protein Levels in the Brain of an Alzheimer's Disease Mouse Model, TASTPM. *J. Photochem. Photobiol. B.* **2013**, *123*, 13–22. [CrossRef]

27. Moro, C.; El Massri, N.; Torres, N.; Ratel, D.; De Jaeger, X.; Chabrol, C.; Perraut, F.; Bourgerette, A.; Berger, M.; Purushothuman, S.; et al. Photobiomodulation inside the Brain: A Novel Method of Applying near-Infrared Light Intracranially and Its Impact on Dopaminergic Cell Survival in MPTP-Treated Mice: Laboratory Investigation. *J. Neurosurg.* **2014**, *120*, 670–683. [CrossRef]
28. Zhang, Q.; Zhou, C.; Hamblin, M.R.; Wu, M.X. Low-Level Laser Therapy Effectively Prevents Secondary Brain Injury Induced by Immediate Early Responsive Gene X-1 Deficiency. *J. Cereb. Blood Flow Metab.* **2014**, *32*, 1391–1401. [CrossRef] [PubMed]
29. Huang, Y.Y.; Chen, A.C.; Carroll, J.D.; Hamblin, M.R. Biphasic Dose Response in Low Level Light Therapy. *Dose-Response* **2009**, *7*, 358–383. [CrossRef]
30. Salehpour, F.; Cassano, P.; Rouhi, N.; Hamblin, M.R.; De Taboada, L.; Farajdokht, F.; Mahmoudi, J. Penetration Profiles of Visible and Near-Infrared Lasers and Light-Emitting Diode Light through the Head Tissues in Animal and Human Species: A Review of Literature. *Photobiomodulation Photomed. Laser Surg.* **2019**, *37*, 581–595. [CrossRef]
31. Rosenberg, N.; Gendelman, R.; Noofi, N. Photobiomodulation of Human Osteoblast-like Cells in Vitro by Low-Intensity-Pulsed LED Light. *FEBS Open Bio* **2020**, *10*, 1276–1287. [CrossRef]
32. Garza, K.M.; Zhang, L.; Borron, B.; Wood, L.B.; Singer, A.C. Gamma Visual Stimulation Induces a Neuroimmune Signaling Profile Distinct from Acute Neuroinflammation. *J. Neurosci.* **2020**, *40*, 1211–1225. [CrossRef]
33. Henderson, T.A.; Morries, L.D. Near-Infrared Photonic Energy Penetration: Can Infrared Phototherapy Effectively Reach the Human Brain? *Neuropsychiatr. Dis. Treat.* **2015**, *11*, 2191–2208. [CrossRef]
34. Ilic, S.; Leichliter, S.; Streeter, J.; Oron, A.; DeTaboada, L.; Oron, U. Effects of Power Densities, Continuous and Pulse Frequencies, and Number of Sessions of Low-Level Laser Therapy on Intact Rat Brain. *Photomed. Laser Surg.* **2006**, *24*, 458–466. [CrossRef] [PubMed]
35. Golovynska, I.; Golovynskyi, S.; Stepanov, Y.V.; Stepanova, L.I.; Qu, J.; Ohulchanskyy, T.Y. Red and Near-Infrared Light Evokes Ca^{2+} Influx, Endoplasmic Reticulum Release and Membrane Depolarization in Neurons and Cancer Cells. *J. Photochem. Photobiol. B Biol.* **2021**, *214*, 112088. [CrossRef] [PubMed]